Elsevier Editorial System(tm) for Atmospheric Research
Manuscript Draft

Manuscript Number:

Title: MICROPHISICAL CHARACTERIZATION OF THE PRECIPITATION IN AMAZON REGION USING RADAR AND DISDROMETER DATA

Article Type: Special Issue: ICCP 2008

Keywords: Radar; Disdrometer; Microphysical data; Raindrop size distributions

Corresponding Author: Rafael Rafael Castelo Guedes Martins, MSc.

Corresponding Author's Institution: FUNCEME

First Author: Rafael Castelo Guedes Martins, MSc.

Order of Authors: Rafael Castelo Guedes Martins, MSc.; Luiz A. T Machado, Dr.; Alexandre A Costa, Dr.

Abstract: One of the most complex problems in atmospheric modeling is the simulation of the microphysical processes related to precipitation production. The representation of such processes becomes more and more important as atmospheric models use increasingly finer resolutions. It occurs in detriment of convective parameterization, which is no longer used as cloud-scale circulations turn out to be resolved. In particular, raindrop size distributions (RDSDs) are an important factor to determine the characteristics of clouds and cloud systems, including their precipitation efficiency and optical properties that may trigger dynamical-microphysical or radiative-dynamical-microphysical feedbacks. This work presents a characterization of the precipitation diurnal cycle through analysis of radar reflectivity profiles and drop-size distributions attained respectively from a microwave vertical profiler and a disdrometer used in the 1999 WET-AMC experiment. In such analysis, precipitation was split in time and classes, which provided information on the daily variation of typical reflectivity profiles and the raindrop spectra associated with them. Statistical analysis revealed that most DSDs exhibit a single peak around 0.5 mm (48.9%), 1.0 mm

(30.7%) or 2.0 mm (2.5%) and that only a few are effectively bimodal, which permitted the use of gamma distributions to fit most of the observed raindrop spectra.

Suggested Reviewers: Ali Tokay Dr
NASA
tokay@radar.gsfc.nasa.gov
he is specialist in Disdrometer data

Tom Rickenbach
He published a paper about precipitation system and types during the WET/AMC experiment.

INPE ePrint: sid.inpe.br/mtc-m18@80/2009/10.06.10.49 v1 2009-10-07

MICROPHISICAL CHARACTERIZATION OF THE PRECIPITATION IN AMAZON REGION USING RADAR AND DISDROMETER DATA

Rafael Castelo Guedes Martins [a,*], Luiz Augusto Toledo Machado [b], Alexandre Araújo Costa [c]

[a] *Fundação Cearense de Meteorologia e Recursos Hídricos - Brazil*
[b] *Instituto Nacional de Pesquisas Espaciais – Brazil*
[c] *Universidade Estadual do Ceará - Brazil*

ABSTRACT

One of the most complex problems in atmospheric modeling is the simulation of the microphysical processes related to precipitation production. The representation of such processes becomes more and more important as atmospheric models use increasingly finer resolutions. It occurs in detriment of convective parameterization, which is no longer used as cloud-scale circulations turn out to be resolved. In particular, raindrop size distributions (RDSDs) are an important factor to determine the characteristics of clouds and cloud systems, including their precipitation efficiency and optical properties that may trigger dynamical-microphysical or radiative-dynamical-microphysical feedbacks. This work presents a characterization of the precipitation diurnal cycle through analysis of radar reflectivity profiles and drop-size distributions attained respectively from a microwave vertical profiler and a disdrometer used in the 1999 WET-AMC experiment. In such analysis, precipitation was split in time and classes, which provided information on the daily variation of typical reflectivity profiles and the raindrop spectra associated with them. Statistical analysis revealed that most DSDs exhibit a single peak around 0.5 mm (48.9%), 1.0 mm (30.7%) or 2.0 mm (2.5%) and that only a few are effectively bimodal, which permitted the use of gamma distributions to fit most of the observed raindrop spectra.

Keywords: Radar; Disdrometer; Microphysical data; Raindrop size distributions

* Corresponding author:
E-mail address: rafael@funceme.br (R.C.G. Martins).

2 – INTRODUCTION

A proper representation of the diurnal modulation of convection is of great importance to improve the skill of atmospheric models used in weather and climate prediction. Because of the corresponding variation in cloud coverage, the diurnal cycle of convection strongly influences the radiative forcing and the energy budget on Earth´s surface.

It is fairly known, however, that cloud processes are highly complex and that their effect is hard to be estimated. Some of the major uncertainties related to cloud processes are due to cloud microphysics, including variations in particle concentration, mean size and size distribution, ice-water partition, existence of different types of ice particles (isolated crystals, aggregates, graupel particles, hailstones) and ice crystal habit variability.

Processes of hydrometeor formation, growth, transformation and precipitation occur on the microphysical scale and the complex series of events that results in a given hydrometeor distribution shows the signature of the environment (Tokay and Short, 1999). In fact, the properties of a cloud ensemble depend on the dynamics and thermodynamics on the large and meso scales as well as on the characteristics of the aerosol field. Therefore, a comprehensive description of the diurnal cycle of convection must include cloud microphysics along with larger scale variables (thermodynamics, cloud coverage, etc.). Understanding the relationship among those variables and their response to the diurnal cycle is essential to quantify the physical mechanisms that organize convection variability. For instance, using radar reflectivity (including differential reflectivity) and vertical velocity data, Yuter and Houze (1995) investigated the microphysics and the kinematics of convective processes in multicell storms during the transition from convective to stratiform precipitation.

Remote sensing studies using radar show that the hydrometeor distributions have a significant impact on the interpretation of data collected remotely (Waldvogel, 1974; Heinrich et al. 1996). Some analyses suggest the coexistence of drop size distributions (DSDs) typical of convective and stratiform regimes within tropical convective systems (Tokay and Short, 1996) and Ferrier et al. (1995) showed that the parameterization of RDSDs in cloud systems, separating the convective and stratiform patterns, improves the performance of atmospheric models.

In this paper, our objective is not to separate convective and stratiform raindrop spectra. Instead, the idea is to use precipitation data collected during the Amazon rainy season using a vertical pointing radar (VPR) and a disdrometer to describe the diurnal variation of the properties of convection. In Section 2, the experiment is described. In section 3, the diurnal variation of radar reflectivity profiles and RDSDs is analyzed and, in Section 4, analytical fittings for the observed raindrop spectra are presented. Concluding remarks, including useful findings for cloud modeling, are shown in Section 5.

2 – EXPERIMENTAL DATA

2.1. The WET-AMC Experiment

WET-AMC/LBA *(WET Atmospheric Mesoscale Campaign / Large Scale Biosphere Atmosphere Experiment in Amazonia)* was held during the months of January and February 1999 over the state of Rondônia, in Southwest Amazon (Figure 1). The campaign focused on the analysis of the local effects of different land uses, the regional convective response to the large-scale forcing and the interaction between convection and biosphere through physical-chemical processes, including the ones related to soil and vegetation (Silva Dias et al., 2002). The present work used data from the vertical pointing radar (VPR) and the disdrometer used during WET-AMC.

2.2. Radar and Disdrometer

The impact disdrometer Joss-Waldvogel (JWD) RD-69 (Joss e Waldvogel, 1967) was installed at the Ji-Paraná airport (latitude 10.88S; longitude 61.81W) in Rondonia state, close to the center of the WET-AMC area shown in Figure 1. The disdrometer classified raindrops in 20 different size classes for 60 s time intervals for a total of 4697 samples and an accumulated rainfall of 288 mm.

The 915 MHz VPR (33cm wavelength) was also installed at the Ji-Paraná airport, close to the disdrometer, obtaining reflectivity profiles with a resolution of 210 m each minute. Data collection started on 17 January and ended on 01 March 1999. Both datasets were processed by Albrecht (2005).

2.3. Methodology

Data from the disdrometer were originally in drops per cubic meter per milimeter ($m^{-3}mm^{-1}$). The concentration of raindrops for each bin in m^{-3} was calculated then, multiplying the original data by the respective bin width. Following, the total concentration in m^{-3} and the precipitation rate (R, in mm h^{-1}) were also determined

In order to investigate diurnal cycle of the precipitation and the corresponding RDSDs, the data were first separated into categories of precipitation intensity using the criterion presented by Tokay and Short (1996), as in Table 1.

In this study, very weak precipitation (i.e., precipitation rates below 1 mm h^{-1}) were not considered, since in those cases the errors in the disdrometer measurements are significant (due to wind, acoustic noise in the environment and oscillations in the disdrometer membrane) and because it is about the minimum for radar detection (20 dBZ). Once divided into precipitation classes, the data were also separated in 4 time periods, each 6 h long, as in Table 2. The time intervals were defined after data inspection, which allowed grouping them based on similar properties of convection.
Disdrometer data from each time interval were averaged to obtain typical raindrop number concentration (m^{-3}), percent raindrop concentration per bin and precipitation rate. Using VPR data, average reflectivity profiles were also calculated for the same time intervals.

3 – ANALYSIS OF THE DIURNAL CYCLE OF PRECIPITATION

3.1 Averages per time interval

Figure 2 summarizes the major characteristics of convection as precipitation events were grouped in the four intervals described in Table 2. Average raindrop concentrations per bin showed peaks around 0.5, 1.0 and 2.0 mm in every time interval (panel 2a). This result suggests that RDSDs may be represented as the superposition of analytical functions with maxima in those diameters. Average reflectivity profiles (panel 2b) reveal well defined characteristics for each time of the day. Intervals centered at 03:00 and 09:00 LST exhibit profiles that are typically stratiform, with a well developed bright band. The profile centered at 15:00 LST shows a marked convective signature with strong precipitation and a well developed ice phase, which is indicated by the highest reflectivity values both in low levels and in upper levels. Finally, the profile observed at 21:00 LST has intermediate characteristics: the presence of high

reflectivity in low levels indicates the permanence of relatively strong convective rainfall but the reduction of upper level reflectivity suggests the collapse of the ice phase. It is also possible to perceive the initiation of the bright band close to the 0°C isotherm.

Properties of the dependence of the precipitation microphysics on the time interval are also shown in panel 2c. Although the raindrop number concentration is fairly constant, the precipitation rate increases by a factor of 4 from 9:00 LST to 15:00 LST, indicating the dominance of larger raindrops accompanying the occurrence of stronger rainfall. This means that for the same average raindrop concentration, one could have either convective precipitation, associated with high radar reflectivity and a RDSD with large raindrops, or stratiform rainfall, with smaller raindrops and reflectivity profiles marked by the presence of the bright band.

3.2. Dependence of VPR Average Profiles on Rainfall Intensity

As shown previously, average VPR profiles suggest the existence of a certain signature of the precipitation type depending on the time interval. This fact becomes more evident as we subdivide those profiles in classes of rainfall intensity.

Figure 3 depicts the reflectivity profiles associated with different classes of precipitation rate in each of the four time intervals. Panel 3a shows that at 03:00 LST, two types of patterns may occur. For the low precipitation classes (1–2 e 2–5 $mm.h^{-1}$), the average profile is predominantly stratiform with a well developed bright band, whereas classes with stronger precipitation exhibit mostly convective characteristics, as larger values of reflectivity in low levels (despite the relatively small values in upper levels and the appearance of a developing bright band). Both panels 3a and 3b correspond to decaying convective activity and in fact panel 3b (09:00 LST) does not show precipitation rates above 5 $mm.h^{-1}$ and both average profiles are typically stratiform. In opposition, in panel 3c (events centered in 15:00 LST), the profiles are strictly convective for all rainfall intensity classes, even though the production of convective rainfall and the presence of ice are obviously more significant in the profiles corresponding to stronger precipitation (as attested by the increased reflectivity in both low and upper levels). The profile corresponding to the extreme precipitation (above 20 $mm\ h^{-1}$) is the one that shows the most developed ice phase, with a significant reduction of this pattern in the other classes. Those profiles are compatible with the onset of

precipitation and the first stages in the evolution of convective systems. At last, panel 3d, corresponding to 21:00 LST, is the one that corresponds to more mature cloud systems, including the persistence of ice and the embryo of the bright band. This profile clearly shows the relationship between ice aloft and precipitation commonly used to estimate precipitation from high microwave frequency over land.

4. FITTING RDSDs TO ANALYTICAL DISTRIBUTIONS

In the previous Section, as the diurnal evolution of precipitation over the Amazon during WET-AMC was described, the average RDSDs tended to exhibit multiple peaks regardless of the time interval (Panel 2a). At a first glance, three maxima could be identified, corresponding to diameters of about 0.5, 1.0 and 2.0 mm.

Then, a closer evaluation of the drop spectra was carried out, dividing the disdrometer observations according to the bin for which the peak concentration occurred. From a total of 4607 spectra, 48.9% showed a peak about 0.5 mm, 30.7% about 1.0 mm and 2.5% about 2.0 mm, which means that 3858 spectra were unimodal, with a single peak about one of those three values. Most of the rest (17.9% of the total) showed peaks about other values and only a few were bimodal. Therefore the multiple peaks shown in panel 2a do not correspond to truly bi or multimodal RDSDs, rather were due to the averaging process, which combined the alternating unimodal RDSDs with peaks predominantly about 0.5, 1.0 and 2.0 mm from different rain rate intensity. Figure 4 depicts the normalized concentration as a function of the diameter for the average of the spectra with peaks about those values.

As more than 82% of the RDSDs are unimodal with peaks around those three values, one can possibly parameterize those size distributions in atmospheric models using analytical fits to only three curves, as far as the shapes of the distributions are not so diverse. Therefore, as several atmospheric models use the gamma distribution as a basis function (e.g., Ferrier 1994, Walko et al. 1995, Meyers et al. 1997), the spectra with peaks around 0.5, 1.0 e 2.0 mm were fitted by such type of distribution.

Fittings were carried out according to Costa et al. (2000). The equation of the gamma distribution is

$$N(D) = \frac{N_t}{\Gamma(\nu)}\left(\frac{D}{D_0}\right)^{\nu-1}\frac{1}{D_0}exp\left(-\frac{D}{D_0}\right), \quad (1)$$

where Γ é is the gamma function, N_t represents the total raindrop concentration, q_l the liquid water content, ρ_w the water density and ν is the shape or width parameter.

In equation (1), D_0 is a scale factor, given by

$$D_0 = \left[6\frac{\Gamma(\nu)}{\Gamma(\nu+3)}\frac{q_l}{\pi\rho_w N_t}\right]^{1/3}. \quad (2)$$

This scale diameter is related to the gamma distribution mean diameter and modal diameter according to:

$$D_0 = \nu\overline{D} \quad (3)$$

and

$$D_0 = (\nu-1)D_{\text{mod}} \quad (4)$$

respectively.

Table 3 shows the mean (plus or minus the standard deviation), median and modal shape parameter for the fitted distributions, as well as the percentage of fittings that passed a Lilliefors (modified Kolmogorov-Smirnov) test (Lilliefors 1967, Wilks 2006) at the 5% level. As the majority of the fittings resulted in shape parameters much greater than 1 (in which case the gamma distribution is simply an exponential function), it is clear that the traditional assumption that raindrop spectra follow Marshall-Palmer (i.e., exponential) distributions is not valid at least for the WET-AMC data set. It should be pointed out, however, that the very high values of the mean shape parameter is generally due to the presence of a few very narrow RDSDs, which best fitting is achieved only using very high values of ν (the same occurred in the analysis of cloud droplet spectra by Costa et al. 2000). Hence, the median and modal shape parameters are also shown, as they are probably best choices for use in atmospheric models.

Figure 5 compares the average of the observed spectra (collect at each 60s) with peaks around 0.5 (panel 5a), 1.0 (5b) and 2.0 mm (5c) against the average of the fittings and the so-called "general fitting", i.e., a single fitting using the median shape parameter, provided, for each case, by Table 2. The Figure suggests that the fitting using a gamma distribution is indeed appropriate to represent the observations (one should notice that the false bimodality in the "general fitting" is an artifact from the irregular size bins used by the disdrometer). The use of a single value of ν (the median) for each group of RDSDs also results in a curve that follows the average of the observed spectra, which is encouraging for modelers that use parameterizations with a single, specified shape parameter (as Walko et al. 1995 and Meyers et al. 1997).

5 – SUMMARY AND CONCLUDING REMARKS

In this work, microphysical characteristics of precipitation over the Amazon were analyzed, based on data collected during the WET-AMC experiment in 1999. One of the most interesting features of the convection revealed by the data is the existence of a clear signature of the diurnal cycle, as certain types of precipitation profiles tend to prevail in certain periods. For instance, stratiform rainfall is dominant for 03:00 e 09:00 LST, following the collapse of the convective structures (which, according to Rickenbach (2003), occur around 22:00 LST, with maximum rainy area and cloud coverage and increase in the stratiform precipitation in detriment of the convective rainfall). This result is also in agreement with Machado et al. (2002) that verified the existence of a maximum rainy area in the S-Pol radar range (see Figure 1 for radar location) about that time as well as maximum cloud coverage during nighttime. Also in agreement with those previous results, the time interval centered at about 21:00 LST shows a transition from convective to stratiform precipitation in every rainfall intensity class, accompanying the collapse of the ice phase and convective activity. The interval centered at 15:00 LST exhibits patterns of reflectivity and raindrop spectra that are typical of the dominance of convective activity, such as the strong reflectivity in lower levels and the development of the ice-phase signature in upper levels.

The analysis of the RDSDs observed via disdrometer during WET-AMC showed that most of them (about 82%) exhibited peaks around 0.5, 1.0 or 2.0 mm, which is consistent with previous results. Steiner and Waldvogel (1987) observed multiple peaks of raindrop concentrations (around 0.7, 1.0, 1.9 and 3.2 mm) and Beauville et al. (1988)

found peaks around 0.6, 1.0, 1.8 e 3.0 mm for tropical convection near the coast. Those observational results reinforce the idea that multiple modes emerge from a precipitation field in steady state as the effect of collision-coalescence ceases, defended by several modelers such as Valdez and Young (1985), List et al. (1987), Hu and Srivastava (1995) and Brown (1989) that found trimodal equilibrium RDSDs.

Finally, we should mention that the observed RDSDs, which are mostly unimodal at the timescale of about one minute, can be fitted to gamma distributions with a high level of statistical confidence (this is equivalent to state that the observed RDSD in a longer timescale can be well fitted via a combination of more than one – for instance, three – gamma distributions with different modal diameters). This contradicts a common assumption that raindrop distributions are nearly exponential and indicated that distribution functions with at least two degrees of freedom (as the gamma distribution) must be used in order to properly represent RDSDs. On the other hand, it was also shown that the number concentration of raindrops is rather constant, even considering different times of the day, and that the use of a single value of the shape parameter may provide a reasonable representation of observed raindrop spectra. Both of those facts indicate that a relatively low level of complexity in bulk microphysical schemes is sufficient to capture important features of the microphysics of precipitation (for instance combining a predicted rainwater mixing ratio with user-specified or diagnosed raindrop number concentration and gamma distribution shape parameter).

ACKNOWLEDGEMENTS: The authors are grateful to the Brazilian Research Council (CNPq) for the master of science fellowship granted to the first author..

6 – REFERENCES

Albrecht, R.I., Silva Dias, M.A.F., 2005. Microphysical evidence of the transition between predominant convective/stratiform rainfall associated with the intraseasonal oscillation in the Southwest Amazon. Acta Amazonica, 35, n2.

Brown, P.S., Jr., 1989. Coalescence and breakup induced oscillations in the evolution of the raindrop size distribution. Journal of the Atmospheric Sciences, 46. 1186-1192.

Costa, A.C., de Oliveira, C.J., de Oliveira, J.C.C., Sampaio, A.J.C., 2000. Microphysical Observations of Warm Cumulus Clouds in Ceará, Brazil, Atmospheric Research, 54, 167-199.

de Beauville, C. A., R. H. Petit, G. Marion, and J. P. Lacaux, 1988. Evolution of peaks in thespectral distribution of raindrops from warm isolated maritime clouds. J. Atmos. Sci., 45, 3320-3332.

Ferrier, B. S., 1994. A double-moment multiple-phase four-class bulk ice scheme. Part I: Description. Journal of the Atmospheric Sciences, 51, 249-280.

Ferrier, B. S., Tao, W.K., Simpson, J., 1995. A double-moment multiple-phase four-class bulk ice scheme. Part II: Simulations of convective storms in different large-scale environments and comparisons with other bulk parameterizations. Journal of the Atmospheric Sciences, 52, 1001–1033.

Heinrich, W., Joss, J., Waldvogel, A., 1996. Raindrop size distributions and the radar bright band. Journal of Applied Meteorology and Climatology, 35, 1688–1701.

Hu, Z., Srivastava, R.C., 1995. Evolution of Raindrop Size Distribution by Coalescence, Breakup, and Evaporation: Theory and Observations. Journal of the Atmospheric Sciences, 52, 1761–1783.

Joss, J., Waldvogel, A., 1967. Ein Spectrograph fur Niedersclagstropfen mit automatisher Auswertung (A spectrograph for the automatic analysis of raindrops), Pure and Applied Geophysics, 68, 240– 246.

Lilliefors, H., 1967. On the Kolmogorov-Smirnov test for normality with mean and variance unknown. Journal of the American Statistical Association, 62, 399-402.

List, R., Donaldson, N.R., Stewart, R.E., 1987.Temporal evolution of drop spectra to collisional equilibrium in steady and pulsating rain. Journal of the Atmospheric Sciences, 44, 362-372.

Machado, L.A.T., Laurent, H., Lima, A.A., 2002. Diurnal march of the convection observed during TRMM-WETAMC/LBA. Journal of Geophysical Research, 107, 1-15.

Marshall, J.S., Palmer, W.Mc., 1948. The Distribution of Raindrops with Size. Journal of Meteorology, 5, 165-166.

Meyers, M. P., Walko, R.L., Harrington, J.Y., Cotton, W.R., 1997. New RAMS cloud microphysics parameterization. Part II: The two-moment scheme. Atmospheric Research, 45, 3-39.

Rickenbach, T.M., 2004. Nocturnal Cloud Systems and Diurnal Variation of Clouds and Rainfall in Southwestern Amazonia. Monthly Weather Review, 132, 1201-1219.

Silva Dias, M.A.F. et al., 2002. Clouds and rain processes in a biosphere-atmosphere interaction context in the Amazon region. Journal of Geophysical Research, 107.

Steiner, M., Waldvogel, A., 1987. Peaks in Raindrop Size Distributions. Journal of the Atmospheric Sciences, 44, 3127–3133.

Tokay, A. and Short, D. A., 1996. Evidence from tropical raindrop spectra of the origin of rain from stratiform versus convective clouds. Journal of Applied Meteorology and Climatology, 35, 355-371.

Tokay, A., Short, D.A., 1999. Tropical Rainfall Associated with Convective and Stratiform Clouds: Intercomparison of Disdrometer and Profiler Measurements. Journal of Applied Meteorology, 38, 302–320.

Valdez, M. P., Young, K.C., 1985. Number Fluxes in Equilibrium Raindrop Populations: A Markov Chain Analysis. Journal of the Atmospheric Sciences, 42, 1024-1036.

Waldvogel, A., 1974. The N_0 jump of raindrop sprectra. Journal of the Atmospheric Sciences, 32, 1068-1078.

Walko, R. L., Cotton, W. R., Meyers, M. P., Harrington, J. Y., 1995. New RAMS cloud microphysics parameterization Part I: the single-moment scheme. Atmospheric Research, 38, 29-62.

Wilks, D. S., 2006. Statistical Methods in the Atmospheric Sciences. 2nd ed. Academic Press, 627 pp.

Yuter, S.E. and Houze, R.A., 1995. Three-Dimensional Kinematic and Evolucion of Florida Cumulunimbus. Part I: Spacial Distribution of Updrafts, Downdrafts, and Precipitation. Monthly Weather Review, 123, 1921-1940.

LIST OF FIGURES AND TABLE

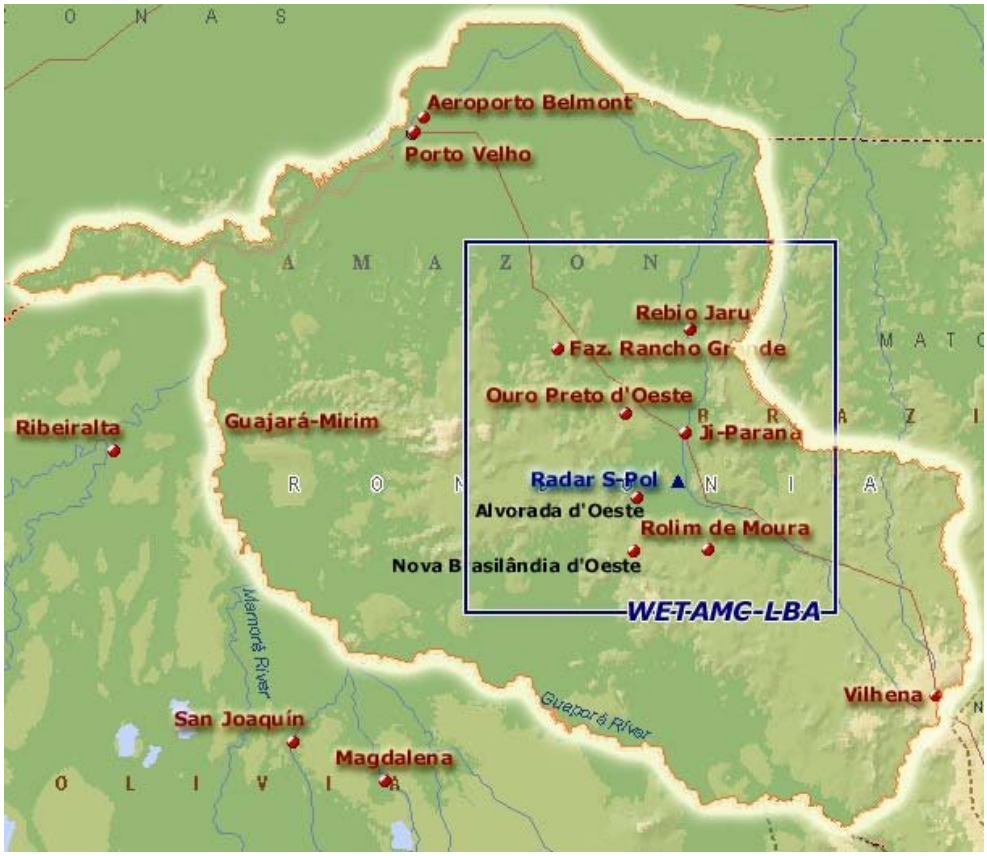

Figure 1 – WET-AMC / LBA experiment sites.

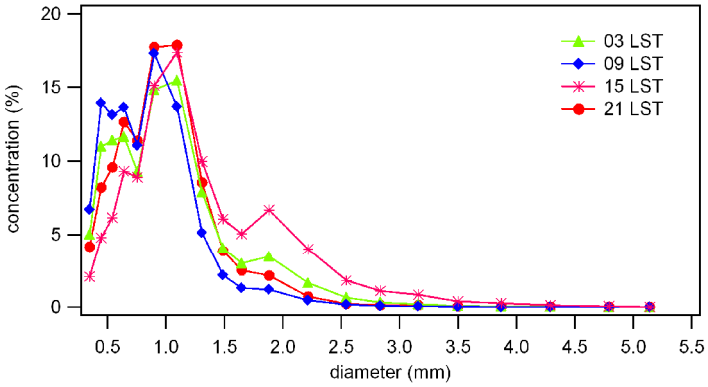

(a)

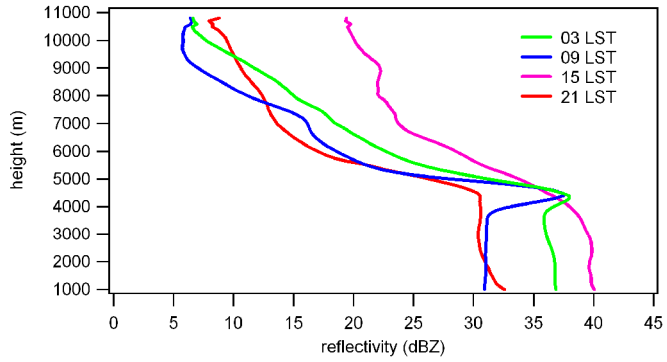

(b)

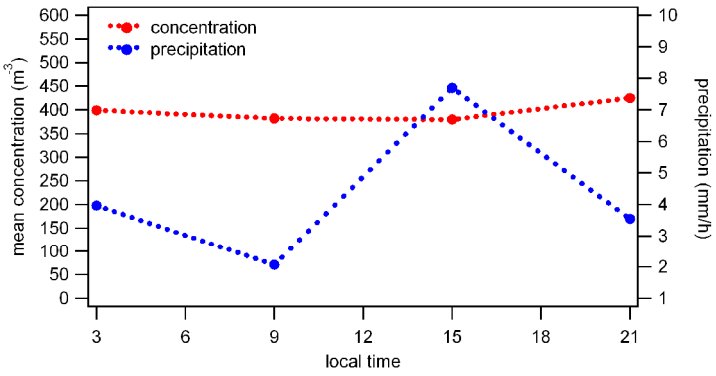

(c)

Figure 2 – (a) Average raindrop concentration per size category (m^{-3}) around 03:00, 09:00, 15:00 and 21:00 LST (b) Average reflectivity profiles around 03:00, 09:00, 15:00 and 21:00 LST (c) Average raindrop number concentration (m^{-3}) and precipitation rate ($mm\ h^{-1}$).

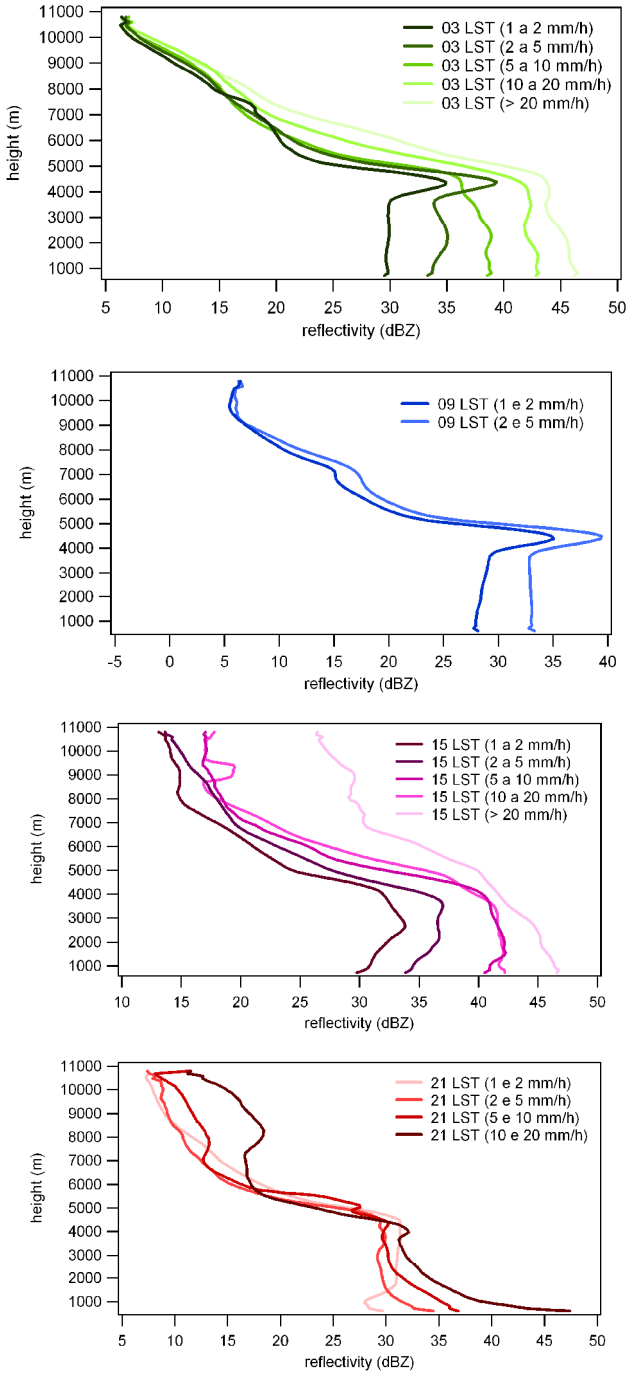

Figure 3 – VPR profiles corresponding to different rainfall intensities and time intervals: (a) 03:00 LST, (b) 09:00 LST, (c) 15:00 LST and (d) 21:00 LST.

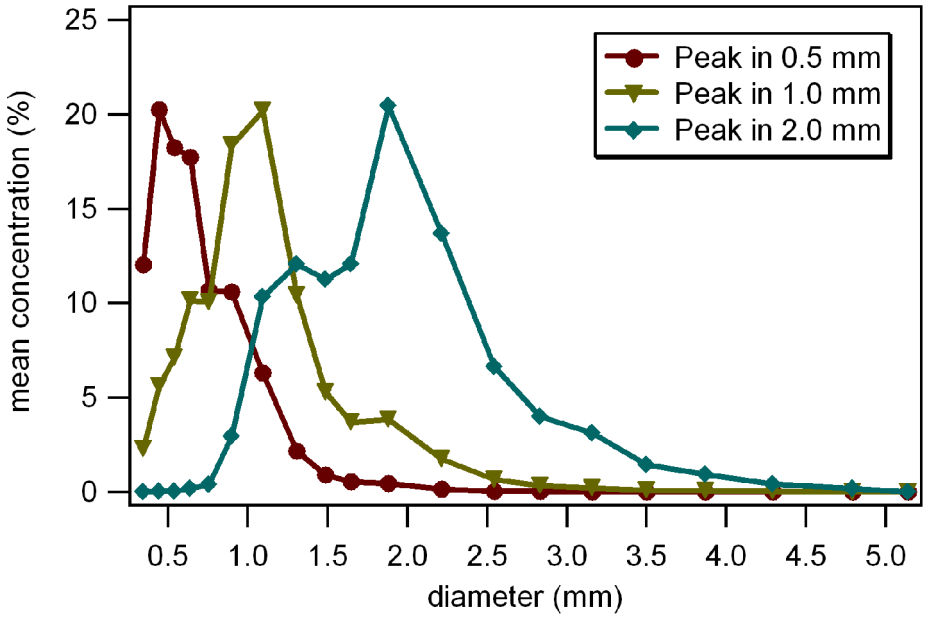

Figure 4 – Normalized concentration as a function of the diameter for the average of the spectra with peaks about 0.5 (red), 1.0 (yellow) e 2.0 mm (blue).

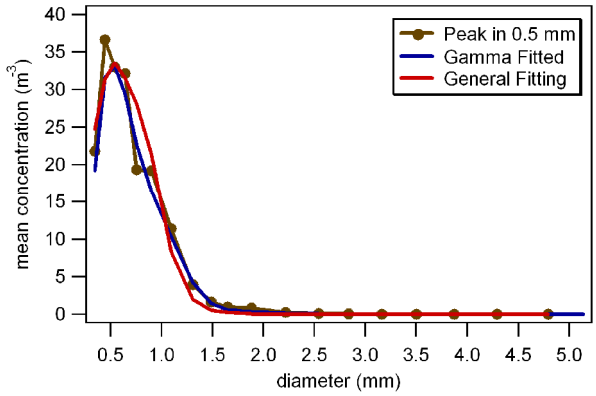

(a)

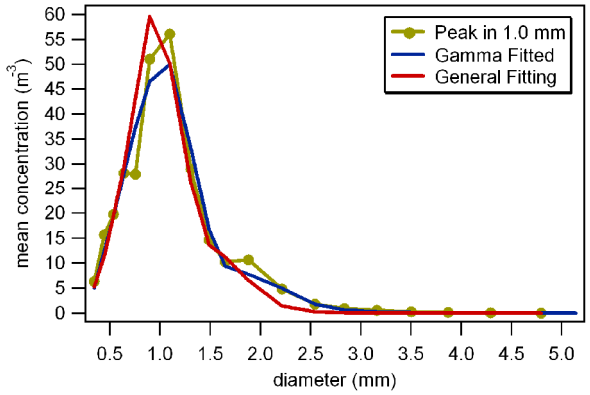

(b)

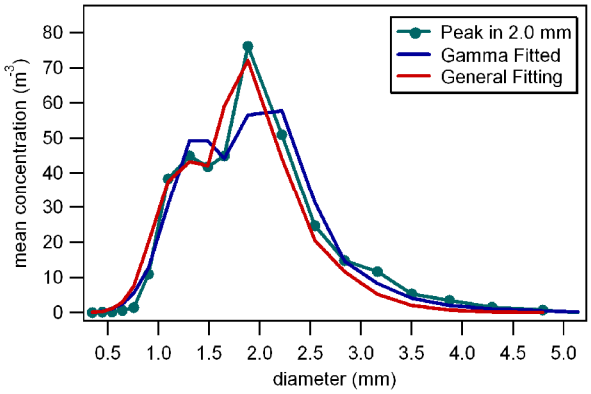

(c)

Figure 5 – Average concentration as a function of the diameter for the spectra with peaks about (a) 0.5, (b) 1.0 and (c) 2.0 mm, compared against the respective average of fittings and the "general fitting" (i.e., the fitting using the median shape parameter for each case).

Table 1 – Precipitation categories

Category	***R (mm h^{-1})***
Very weak	$R < 1$
Weak	$1 \leq R < 2$
Moderate	$2 \leq R < 5$
Strong	$5 \leq R < 10$
Very strong	$10 \leq R < 20$
Extreme	$R \geq 20$

Table 2 – Time intervals for diurnal cycle analysis

Local Standard Time (LST)
[00:00 LST - 05:59 LST] centered on 03:00 LST
[06:00 LST - 11:59 LST] centered on 09:00 LST
[12:00 LST - 17:59 LST] centered on 15:00 LST
[18:00 LST - 23:59 LST] centered on 21:00 LST

Table 3 – Gamma fittings statistics: mean (with standard deviation), median and modal shape parameter for distributions with peaks in 0.5, 1.0 and 2.0 mm. The percentage of fittings that passed the KS test is also shown.

Shape parameter	*Peak in 0.5 mm*	*Peak in 1.0 mm*	*Peak in 2.0 mm*
ν_{mean} **(± s.d.)**	7.5 ± 4.4	9.1 ± 5.5	9.6 ± 3.3
ν_{median}	6.1	7.1	9.2
ν_{modal}	5 – 6	5 - 6	9 - 10
Percentage that passed the KS test (5%)	**84.2%**	**86.3%**	**94.1%**